



HAL
open science

Second-Sphere Biomimetic Multipoint Hydrogen-Bonding Patterns to Boost CO₂ Reduction of Iron Porphyrins

Philipp Gotico, Bernard Boitrel, Régis Guillot, Marie Sircoglou, Annamaria Quaranta, Zakaria Halime, Winfried Leibl, Ally Aukauloo

► **To cite this version:**

Philipp Gotico, Bernard Boitrel, Régis Guillot, Marie Sircoglou, Annamaria Quaranta, et al.. Second-Sphere Biomimetic Multipoint Hydrogen-Bonding Patterns to Boost CO₂ Reduction of Iron Porphyrins. *Angewandte Chemie International Edition*, 2019, 58 (14), pp.4504-4509. 10.1002/anie.201814339 . hal-02050269

HAL Id: hal-02050269

<https://univ-rennes.hal.science/hal-02050269>

Submitted on 13 Mar 2019

HAL is a multi-disciplinary open access archive for the deposit and dissemination of scientific research documents, whether they are published or not. The documents may come from teaching and research institutions in France or abroad, or from public or private research centers.

L'archive ouverte pluridisciplinaire **HAL**, est destinée au dépôt et à la diffusion de documents scientifiques de niveau recherche, publiés ou non, émanant des établissements d'enseignement et de recherche français ou étrangers, des laboratoires publics ou privés.

Second-Sphere Biomimetic Multipoint Hydrogen-Bonding Patterns to Boost CO₂ Reduction of Iron Porphyrins

Philipp Gotico, Bernard Boitrel, Régis Guillot, Marie Sircoglou, Annamaria Quaranta, Zakaria Halime,* Winfried Leibl, and Ally Aukauloo*

Abstract: Inspired by nature's orchestra of chemical subtleties to activate and reduce CO₂, we have developed a family of iron porphyrin derivatives in to which we have introduced urea groups functioning as multipoint hydrogen-bonding pillars on the periphery of the porphyrinic ring. This structure closely resembles the hydrogen-bond stabilization scheme of the carbon dioxide (CO₂) adduct in the carbon monoxide dehydrogenase (CODH). We found that such changes to the second coordination sphere significantly lowered the overpotential for CO₂ reduction in this family of molecular catalysts and importantly increased the CO₂ binding rate while maintaining high turnover frequency (TOF) and selectivity. Entrapped water molecules within the molecular clefts were found to be the source of protons for the CO₂ reduction.

The criticality of global warming effects arising from increasing emission of carbon dioxide (CO₂) is challenging scientists to advance research in the development of catalysts that can help capture, activate, and reduce CO₂. An emphasis is currently being put on the discovery of new cost-efficient molecular catalysts to drive the electrocatalysis of CO₂ reduction and ultimately to use solar energy to drive these energetically uphill chemical transformations.^[1-9] Still, the route towards industrial upscale applications requires much improvement in the efficiency of these catalysts while maintaining their stability and selectivity.

Rational strategies for catalyst design and improvement hinge on what we continually learn from natural systems, as they exhibit exceptional stabilities and performance. Carbon monoxide dehydrogenase (CODH) stands as the typical inspiration for scientists working on the field as it is known to catalyze the reversible reduction of CO₂ to CO. Lessons from

the structure and functions of this enzyme point out to some important findings that can be artificially mimicked by catalyst design: 1) a bifunctional activation of CO₂ substrate by two metal centers, 2) an iron-sulfur cluster acting as an electronic relay and buffer to the catalytic unit and 3) precisely positioned amino acid residues to form a hydrogen-bond stabilization network with the CO₂ substrate.^[10-12] Implementing these functionalities in the second coordination sphere^[5] such as local proton source, (i.e. phenols,^[13-15] carboxylic acids^[16]), H-bond donors (amines,^[17] amides,^[18] guanidine^[19]) and reaction intermediate stabilizers (ammonium cations,^[20] and imidazolium moieties^[21,22]) have successfully lead to decrease significantly the overpotential while improving the catalytic turnover numbers (TONs) and frequencies (TOFs).

Inspired by the multipoint hydrogen bonding scheme of histidine (H₉₃) and lysine (K₅₆₃) residues in stabilizing the CO₂ adduct in CODH, we reasoned to introduce urea functions on the periphery of an iron porphyrin, known as one of the most efficient molecular catalysts for the two-electron two-proton reduction of CO₂ to CO. These functions hold two potential NH fragments that can interact with metal bound CO₂. Reed and co-workers first reported the use of a picket-fence porphyrin with a modified phenyl-urea arm in establishing a hydrogen bond to molecular oxygen and improve the substrate affinity of the complex.^[23] Das et al. have shown a crystallographic structure of a neutral urea scaffold that fixes atmospheric CO₂ as carbonate clusters held together by an extended H-bonding stabilization.^[24] Neumann and co-workers have recently reported a thiourea tether placed on the second coordination sphere of a rhenium catalyst that improved the electrocatalytic activity in the absence of external proton source.^[25] However, the presence of weak acids, such as water, inhibits the activity of the latter system which will be problematic when aligning with the sustainable goal of using water as a free source of electrons and protons. During the course of this study, Chang and Nichols have leveraged this multi-point hydrogen bond donation of urea as an external additive to improve the electrocatalytic activity of nickel cyclam at the same overpotential.^[26]

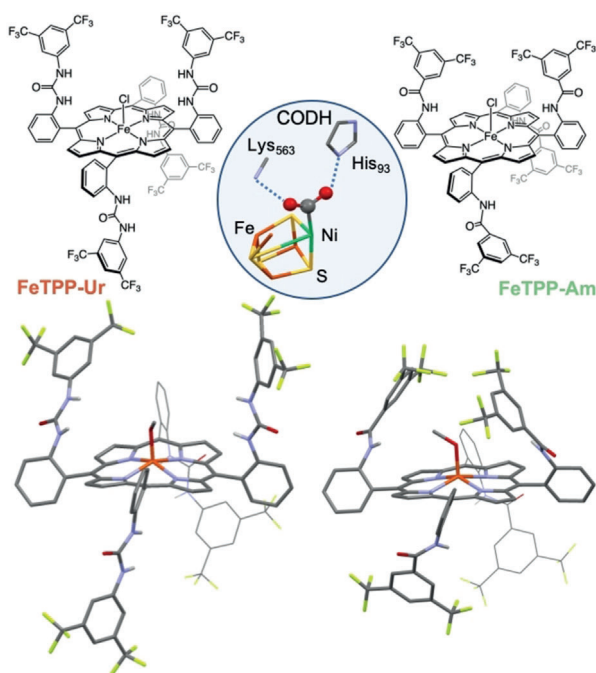
We report herein the synthesis of two super-structured iron porphyrins holding in one case four amido groups (**FeTPP-Am**) and in another four urea functions (**FeTPP-Ur**) (Scheme 1). Both functions carried a phenyl ring bearing two -CF₃ motifs as electron withdrawing groups to enhance hydrogen bonding aptitude of the NH fragments. These two catalysts were designed starting from a 5,10,15,20-tetrakis(2-aminophenyl)porphyrin (**TAPP**) with an $\alpha\beta\alpha\beta$ configuration (Scheme 1). Unlike studies utilizing hangman,^[18,19] and

[*] P. Gotico, Dr. A. Quaranta, Dr. W. Leibl, Prof. A. Aukauloo
Institut de Biologie Intégrative de la Cellule (I2BC), Institut des
Sciences du Vivant Frédéric-Joliot, CEA Saclay
91191 Gif-sur-Yvette (France)
E-mail: ally.aukauloo@u-psud.fr

Dr. B. Boitrel
Univ Rennes, CNRS, ISCR (Institut des Sciences Chimiques de
Rennes)
UMR 6226, Rennes F-35000 (France)

Dr. R. Guillot, Dr. M. Sircoglou, Dr. Z. Halime, Prof. A. Aukauloo
Institut de Chimie Moléculaire et des Matériaux d'Orsay (ICMMO)
UMR 8182 CNRS, Université Paris Sud
91405 Orsay (France)
E-mail: zakaria.halime@u-psud.fr

Supporting information and the ORCID identification number(s) for
the author(s) of this article can be found under:
<https://doi.org/10.1002/anie.201814339>.



Scheme 1. Molecular drawing of **FeTPP-Ur** (top left) and **FeTPP-Am** (top right) and the wireframe and capped sticks representation of their corresponding X-ray structures (**FeTPP-Ur**: bottom left; **FeTPP-Am**: bottom right) with a methoxide anion as an axial ligand. Only urea and amide protons are explicitly shown, and solvent molecules are omitted for clarity. The X-ray structure of the FeNi active site (C-cluster) of CO dehydrogenase (CODH)^[10] (center) is shown for comparison.

picket-fence^[13,22] structures of porphyrins for CO₂ reduction, this atropisomer was chosen with the target to provide two sets of hydrogen bonding network in a *trans* fashion towards a metal bound CO₂ molecule and at the same time to confer two identical chemical faces on each side of the porphyrin molecular platform. Our results showed that the **FeTPP-Am** catalyst had no marked enhancement on the electrocatalytic activity of CO₂ reduction when compared to the tetraphenylporphyrin (**FeTPP**) derivative. Interestingly, the urea containing catalyst **FeTPP-Ur** showed 302 mV positive shift in the catalytic potential for the selective reduction of CO₂ to CO while concomitantly retaining the catalytic performance (TONs and TOFs) of **FeTPP** functioning at much higher overpotential. Furthermore, water was found to be a sufficient and better proton source in CO₂-saturated dimethylformamide (DMF) in comparison with more acidic trifluoroethanol (TFE) and phenol (PhOH).

The synthetic route leading to our target catalysts is depicted in the supplementary information (Figure S1). In short, the addition of four equivalents of 3,5-bis(trifluoromethyl)phenyl isocyanate or 3,5-bis(trifluoromethyl)benzoyl chloride to **TAPP** $\alpha\beta\alpha\beta$ ^[27,28] leads, respectively to porphyrin ligands bearing four urea (**TPP-Ur**) or four amido (**TPP-Am**) groups. Iron insertion in these ligands was performed using ferrous bromide and 2,6-lutidine. X-ray diffraction analyses were obtained for both catalysts **FeTPP-Ur** and **FeTPP-Am**. The preservation of the $\alpha\beta\alpha\beta$ configuration was confirmed by the disposition of the tethered **Ur** and **Am** arms on the

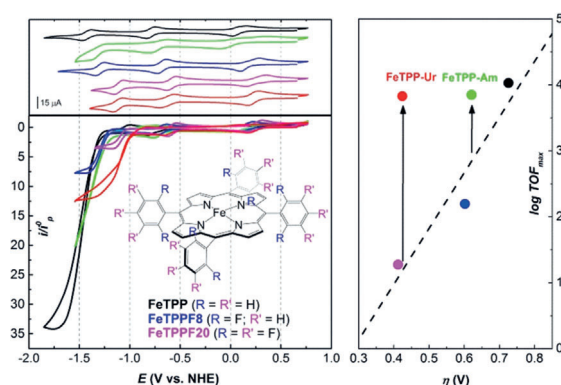


Figure 1. Cyclic voltammograms of 1 mM **FeTPP** (black) and its modified analogues (blue = **FeTPPF₈**, pink = **FeTPPF₂₀**, green = **FeTPP-Am**, red = **FeTPP-Ur**) in DMF containing 0.1 M [Bu₄N]PF₆ at 25 °C under argon (top left) and under CO₂ with 5.5 M water as proton source (bottom left). Plot of calculated TOF_{max} (from FOW analysis) as a function of catalytic overpotential (right, see Supporting Information for calculation details).

periphery of the porphyrin skeleton (Figure 1 and Supporting Information for a more detailed description of the structures). For both complexes, the distances around the iron (III) center best fit with a high spin configuration with an axial methoxide ligand. Of note, the hydrogen atoms of the amido and the urea groups are oriented towards the iron catalytic center, with Fe...H distances of 4.840 Å for the amido groups and from 4.796 to 5.970 Å for both hydrogen atoms of the urea groups, presaging potential hydrogen bond interactions with CO₂ adduct coordinated to the metal center. An interesting structural feature of the **FeTPP-Ur** is the presence of entrapped water molecules in the vicinity of the urea functions (Figure S22).

Cyclic voltammograms (CV) of **FeTPP-Ur** in argon-degassed DMF containing 0.1M of tetra-*N*-butylammonium hexafluorophosphate ([Bu₄N]PF₆) showed three reversible redox waves at 0.226, -0.632, and -1.118 V versus the normal hydrogen electrode (NHE) corresponding, respectively to the formal Fe^{III/II}, Fe^{II/I}, Fe^{I/0} couples (Figure 1, Table S1). All three waves show an anodic shift when compared to those of the non-functionalized iron porphyrin (**FeTPP**) under similar experimental conditions. However, the third redox wave is markedly shifted over 300 mV to more positive potential, a shift similar to that of **FeTPPF₂₀**, a **FeTPP** analogue where all the twenty aryl positions are directly fluorinated (Figure 1, Table S1). This substantial shift cannot be attributed only to the withdrawing inductive effect of the two -CF₃ groups on the aryl ring at the other end of the urea functions. In the case of **FeTPP-Am** holding the same fluorinated substituted aryl groups, only small anodic shift was noted. Instead, the observation can be attributed to the strong electron delocalization on the urea groups helping to contain the addition of electron on the catalytic unit.

The CVs of reference complexes **FeTPP** and the fluorinated analogues **FeTPPF₈** and **FeTPPF₂₀** in CO₂-saturated solution show a catalytic current on the third reduction wave corresponding to the catalytic 2-electron reduction of CO₂ to CO (Figure 1). As discussed previously by Costentin and

Savéant, the counterpart of lowering the overpotential ($\eta = E_{\text{cat}}^0 - E_{\text{CO}_2/\text{CO}}^0$), through classic incorporation of electron withdrawing groups, leads to a decrease in the TOF of the catalysts (Figure 1 right and Table 1).^[5] An escape from this iron law was exemplified with catalysts having a local proton source or favorable second-sphere interactions.^[13–20,22] In the

Table 1: Electrochemical properties of the modified iron porphyrins.

Complex	E_{cat}^0 [a]	η (V) [b]	$\log \text{TOF}_{\text{max}}$ [c]	k_{CO_2} ($\text{M}^{-1} \text{s}^{-1}$) [d]
FeTPP	−1.420	0.73	4.03	7.6
FeTPP-Am	−1.315	0.63	3.85	6.8
FeTPPF₈	−1.296	0.61	2.20	–
FeTPPF₂₀	−1.106	0.42	1.27	–
FeTPP-Ur	−1.118	0.43	3.83	58.0

[a] The catalytic potential, E_{cat}^0 , is taken as the standard reduction potential for the formal $\text{Fe}^{I/0}$ couple (V vs. NHE). [b] Overpotential values are reported as the difference between the E_{cat}^0 and $E_{\text{CO}_2/\text{CO}}^0 = 0.69$ V vs. NHE.^[29] [c] TOF_{max} values are reported for a CO_2 -saturated DMF solution containing 5.5 M H_2O based on FOW analysis. [d] CO_2 binding rate constant is estimated based on reported method^[30] considering irreversible kinetics upon CO_2 binding in dry DMF (see Supporting Information for details).

case of **FeTPP-Am**, in which hydrogen-bond interaction with amide groups can be expected, only a small positive deviation is observed. This positive deviation is much more pronounced in the case of **FeTPP-Ur** catalyst which has comparable TOF to that of **FeTPP** at ca. 300 mV more positive E_{cat}^0 . These comparative studies indicate that the significant enhancement in **FeTPP-Ur** can be assigned to the multipoint hydrogen bonding induced by the urea groups. In a controlled experiment, the addition of an excess of urea as an external additive during the catalytic reduction of CO_2 by **FeTPP** did not bring any improvement to neither the catalytic current nor the E_{cat}^0 (Figure S11). This result underlines the important aspect of the 3D pre-organization of the **FeTPP-Ur** catalyst which places the two urea groups on one side of the porphyrin platform in a position where all four hydrogen atoms of the urea groups can establish hydrogen bonding interactions with a CO_2 substrate on the metal-center from two opposite *meso*-positions of the porphyrin macrocycle. This result is a clear demonstration on the positioning of the hydrogen bonding patterns for optimizing the electrocatalytic properties of our biomimetic designed catalyst **FeTPP-Ur**. It is not the sum of the additional NH interactions as compared to **FeTPP-Am** derivative, but should rather be considered as a close mimic of the lysine and histidine residues of CODH active site. Indeed, based on the structure/function proposal, this pair of amino acids conspires to stabilize a carboxylate intermediate (M-CO_2) through multipoint hydrogen bonding.^[10]

Our choice of introducing urea groups in the second coordination sphere of an iron-porphyrin catalyst was motivated by their ability to bind oxygen atoms of carbonyl groups as well as carbonates.^[31–33] In some cases, urea groups can even capture atmospheric CO_2 as carbonates/bicarbonate.^[24] X-ray structures resolved from single crystals obtained by slow evaporation of H_2O /acetone saturated solution of **TPP-Ur** porphyrin, revealed the presence of four acetone molecules

bound to the four urea groups through $\text{N-H}\cdots\text{O}=\text{C}$ hydrogen bonding interactions (Figure S21), confirming the stabilization of the carbonyls by urea moieties.

To assess the contribution of the urea arms to the binding affinity of CO_2 , we performed the CV of **FeTPP-Ur** under CO_2 but in the absence of a proton source. In these conditions, where the catalytic 2-electron and 2-proton reduction of CO_2 is not possible, we observe both a loss of reversibility and an anodic shift of the third reduction wave (Figure S18a). These characteristics are unprecedented for iron-porphyrin catalysts but were reported as indicative of a good CO_2 binding for other macrocyclic catalysts.^[34,35] For a thorough comparison, the CO_2 binding rate constant (see Supporting Information for details) of **FeTPP-Ur** was estimated and found to be an order of magnitude higher than that of reference compounds such as **FeTPP** or even **FeTPP-Am** (Table 1).

However, this CO_2 binding magnitude may not be the only parameter to account for the high catalytic performance of **FeTPP-Ur**. As mentioned above, a stabilization of reactive intermediates such as Fe-CO_2 species through hydrogen bonding interactions with the NH of urea groups may also contribute. To back up this hypothesis, density functional theory (DFT) calculations were performed on model compounds to investigate on the possible geometry of the CO_2 adducts of the triply reduced iron porphyrins. In the case of **FeTPP-Am**, only two weak hydrogen bonding interactions between the amide arms and the coordinated CO_2 substrate were found with $\text{N(H)}\cdots\text{O}$ donor–acceptor distances of 3.021 and 3.352 Å. In marked contrast, two strong hydrogen bonds were engaged by each urea arms of **FeTPP-Ur** yielding four short $\text{N(H)}\cdots\text{O}$ distances of 2.738, 2.804, 2×2.832 Å (Figure 2 and Figure S32) comparable to those evidenced in the active site of the CODH (2.637 and 2.884 Å with Lys and His residue, respectively). This multipoint anchoring of CO_2 is responsible of a free enthalpy of stabilization of 29 kcal mol^{-1} .

We further interrogated the proton source, a pre-requisite in the reduction of CO_2 . A 5.77 normal kinetic isotope effect (KIE) was measured for the electrocatalytic reduction of CO_2 by **FeTPP-Ur** with $\text{H}_2\text{O}/\text{D}_2\text{O}$ as a proton source indicating that proton transfer is involved in the rate determining step (Figure S20). We then extended this study to other sources of proton currently used in this field, that is, trifluoroethanol (TFE) and phenol (PhOH), by comparing the catalytic rates estimated from the foot of the wave (FOW) analysis.

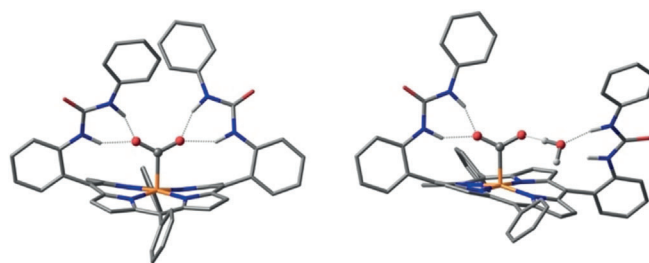


Figure 2. Notional model structures of $[\text{FeTPP-Ur-CO}_2]^{2-}$ (left) and $[\text{FeTPP-Ur-CO}_2]^{2-}$ with a trapped water molecule (right) optimized by DFT calculation at BP86/Def2-SVP(Fe)-6-31 + G(d,p) (other atoms) level of theory. Hydrogen atoms bound to carbon omitted for clarity. H white, C gray, N blue, O red; Fe orange.

Although H₂O is less acidic ($pK_a = 31.5$) than TFE ($pK_a = 24.0$) or PhOH ($pK_a = 18.8$),^[36] surprisingly, it has by far the most marked effect on improving the catalytic rate compared to phenol or TFE (Figure S10).^[36]

Our result is in sharp contrast with a recent study, where the authors observed a severe drop in the catalytic rate upon addition of H₂O or PhOH for a thiourea-tethered rhenium catalyst.^[25] Reasons for this were supported by their DFT calculations suggesting that external protons may disrupt the pre-established hydrogen bond stabilization of the thiourea moiety with the CO₂ adduct. In the case of **FeTPP-Ur**, water seems to work in synergy with the urea arms to manage the proton supply. Support for this proposal come from the network of water molecules observed in the X-ray structure of **FeTPP-Ur** (Figure S22) suggesting that such a network may also be in play during the catalytic reduction of CO₂. A similar water network in the vicinity of the active site of CODH revealed by high resolution X-ray structure was proposed to have a major role in the enzyme reactivity.^[10] The geometry of a model structure where a water molecule was inserted in between a urea arm of **FeTPP-Ur** and CO₂ could be optimized by DFT calculation as a local minimum (Figure 2 right). This configuration is similarly observed for one of the water molecules in the X-ray structure of **FeTPP-Ur** (O₄ in Figure S22). In contrast with the previously mentioned thiourea-tethered Re catalyst, the CO₂ is in this case maintained in a quasi-unchanged topology while being put in contact with a water molecule held by the second urea arm. The less important effect of PhOH and TFE can be due to 1) their higher acidity which can prevent the formation of pre-established intramolecular hydrogen bonds between urea groups and CO₂ adduct, and/or 2) their steric hindrance which can limit their access to the catalytic center in between the two urea arms.

Bulk electrolysis experiment was performed on **FeTPP-Ur** at -1.076 V versus NHE to measure the efficiency at which CO is produced and to evaluate the stability of the catalyst. Gas chromatography analysis of the reaction head-space during bulk electrolysis showed no hydrogen formation and the catalyst **FeTPP-Ur** operates with the exclusive formation of CO with a Faradaic efficiency as high as 91 % (Figure 3). A stable current density of 0.70 mA cm^{-2} was achieved during the two-hour electrolysis run (Figure S12a) which confirms the good stability of the catalyst. Considering a two-electron process, the rate constant (k_{cat}) was calculated to be $2.76 \times 10^3 \text{ s}^{-1}$, the TOF to be 455 s^{-1} , and the TON to be 3.28×10^6 based on the amount of catalyst molecules in the diffusion layer of the working electrode (see Supporting Information for details). As shown in Figure S9, this calculated TOF value fits well in the catalytic Tafel plot of **FeTPP-Ur**, and further points to the distinct advantages of **FeTPP-Ur** over other modified iron porphyrins employing the second coordination effect.

In this study, we have described a biomimetic model containing urea functions that provide a multipoint hydrogen-bonding scheme to bind and stabilize CO₂ for its reduction to CO at an iron porphyrin catalytic unit. Our results clearly demonstrate a remarkable drop in the overpotential in comparison to single-point hydrogen-bonding models while

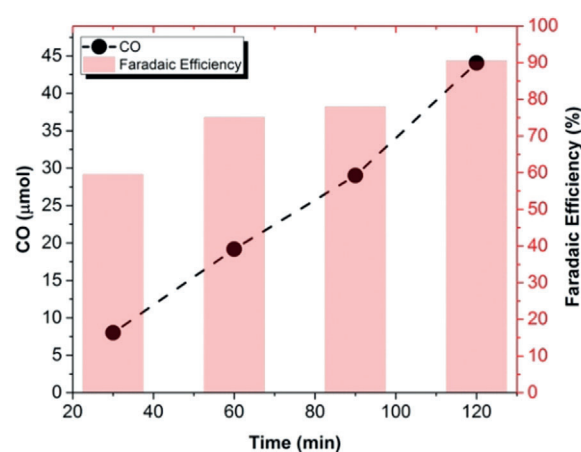


Figure 3. Progress of CO evolution and the corresponding Faradaic efficiency during bulk electrolysis experiments at -1.076 V versus NHE of a CO₂-saturated DMF solution containing 0.5 mM **FeTPP-Ur** and 5.5 M H₂O.

conserving a high turnover frequency. Such a functionality inspired by the active site of carbon monoxide dehydrogenase, is a significant and versatile tool in the design of synthetic cost-effective catalysts. We also found that within such molecular clefts, water was sufficient as a proton source, indicating a future prospect of using water as a sustainable proton and electron source, when coupled to a water oxidizing component.

Acknowledgements

This work was supported by CEA IRTELIS PhD fellowship program (for P.G.), LabEx CHARMMMAT, and by the French Infrastructure for Integrated Structural Biology (FRISBI) ANR-10-INSB-05-01. Prof. V. Gandon is warmly acknowledged for his advices regarding DFT calculation.

Conflict of interest

The authors declare no conflict of interest.

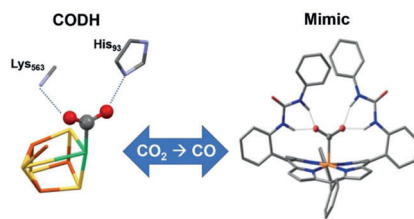
Keywords: carbon dioxide reduction · hydrogen bonding · iron · porphyrins · urea

- [1] J. Hawecker, J.-M. Lehn, R. Ziessel, *Helv. Chim. Acta* **1986**, *69*, 1990–2012.
- [2] V. S. Thoi, C. J. Chang, *Chem. Commun.* **2011**, *47*, 6578–6580.
- [3] M. D. Sampson, A. D. Nguyen, K. A. Grice, C. E. Moore, A. L. Rheingold, C. P. Kubiak, *J. Am. Chem. Soc.* **2014**, *136*, 5460–5471.
- [4] H. Takeda, C. Cometto, O. Ishitani, M. Robert, *ACS Catal.* **2017**, *7*, 70–88.
- [5] C. Costentin, J.-M. Savéant, *Nat. Rev. Chem.* **2017**, *1*, 0087.
- [6] F. Wang, *ChemSusChem* **2017**, *10*, 4393–4402.

- [7] D. Hong, Y. Tsukakoshi, H. Kotani, T. Ishizuka, T. Kojima, *J. Am. Chem. Soc.* **2017**, *139*, 6538–6541.
- [8] Y. Tamaki, O. Ishitani, *ACS Catal.* **2017**, *7*, 3394–3409.
- [9] T. Ouyang, H.-J. Wang, H.-H. Huang, J.-W. Wang, S. Guo, W.-J. Liu, D.-C. Zhong, T.-B. Lu, *Angew. Chem. Int. Ed.* **2018**, *57*, 16480–16485; *Angew. Chem.* **2018**, *130*, 16718–16723.
- [10] J.-H. Jeoung, H. Dobbek, *Science* **2007**, *318*, 1461.
- [11] A. M. Appel, J. E. Bercaw, A. B. Bocarsly, H. Dobbek, D. L. DuBois, M. Dupuis, J. G. Ferry, E. Fujita, R. Hille, P. J. A. Kenis, et al., *Chem. Rev.* **2013**, *113*, 6621–6658.
- [12] M. Can, F. A. Armstrong, S. W. Ragsdale, *Chem. Rev.* **2014**, *114*, 4149–4174.
- [13] C. Costentin, S. Drouet, M. Robert, J.-M. Savéant, *Science* **2012**, *338*, 90–94.
- [14] C. Costentin, G. Passard, M. Robert, J.-M. Savéant, *Proc. Natl. Acad. Sci. USA* **2014**, *111*, 14990–14994.
- [15] C. Costentin, M. Robert, J.-M. Savéant, A. Tatin, *Proc. Natl. Acad. Sci. USA* **2015**, *112*, 6882–6886.
- [16] G. Neri, I. M. Aldous, J. J. Walsh, L. J. Hardwick, A. J. Cowan, *Chem. Sci.* **2016**, *7*, 1521–1526.
- [17] A. Chapovetsky, M. Welborn, J. M. Luna, R. Haiges, T. F. Miller, S. C. Marinescu, *ACS Cent. Sci.* **2018**, *4*, 397–404.
- [18] E. M. Nichols, J. S. Derrick, S. K. Nistanaki, P. T. Smith, C. J. Chang, *Chem. Sci.* **2018**, *9*, 2952–2960.
- [19] C. G. Margarit, C. Schnedermann, N. G. Asimow, D. G. Nocera, *Organometallics* **2018**, <https://doi.org/10.1021/acs.organomet.8b00334>.
- [20] I. Azcarate, C. Costentin, M. Robert, J.-M. Savéant, *J. Am. Chem. Soc.* **2016**, *138*, 16639–16644.
- [21] S. Sung, D. Kumar, M. Gil-Sepulcre, M. Nippe, *J. Am. Chem. Soc.* **2017**, *139*, 13993–13996.
- [22] A. Khadhraoui, P. Gotico, B. Boitrel, W. Leibl, Z. Halime, A. Aukauloo, *Chem. Commun.* **2018**, *54*, 11630–11633.
- [23] G. E. Wuenschell, C. Tetreau, D. Lavalette, C. A. Reed, *J. Am. Chem. Soc.* **1992**, *114*, 3346–3355.
- [24] U. Manna, S. Kayal, S. Samanta, G. Das, *Dalton Trans.* **2017**, *46*, 10374–10386.
- [25] E. Haviv, D. Azaiza-Dabbah, R. Carmieli, L. Avram, J. M. L. Martin, R. Neumann, *J. Am. Chem. Soc.* **2018**, *140*, 12451–12456.
- [26] E. M. Nichols, J. S. Derrick, S. K. Nistanaki, P. T. Smith, C. J. Chang, *Chem. Sci.* **2018**, *9*, 2952–2960.
- [27] J. P. Collman, R. R. Gagne, C. Reed, T. R. Halbert, G. Lang, W. T. Robinson, *J. Am. Chem. Soc.* **1975**, *97*, 1427–1439.
- [28] J. P. Collman, R. R. Gagne, T. R. Halbert, J. C. Marchon, C. A. Reed, *J. Am. Chem. Soc.* **1973**, *95*, 7868–7870.
- [29] C. Costentin, S. Drouet, M. Robert, J.-M. Savéant, *J. Am. Chem. Soc.* **2012**, *134*, 11235–11242.
- [30] J. M. Savéant, in *Elements of Molecular and Biomolecular Electrochemistry*, Wiley, Hoboken, **2006**, pp. 78–181.
- [31] B. H. M. Snellink-Ruël, M. M. G. Antonisse, J. F. J. Engbersen, P. Timmerman, D. N. Reinhoudt, *Eur. J. Org. Chem.* **2000**, 165–170.
- [32] P. R. Schreiner, *Chem. Soc. Rev.* **2003**, *32*, 289–296.
- [33] Z. Zhang, P. R. Schreiner, *Chem. Soc. Rev.* **2009**, *38*, 1187–1198.
- [34] J. Schneider, H. Jia, J. T. Muckerman, E. Fujita, *Chem. Soc. Rev.* **2012**, *41*, 2036–2051.
- [35] C. Cometto, L. Chen, P.-K. Lo, Z. Guo, K.-C. Lau, E. Anxolabéhère-Mallart, C. Fave, T.-C. Lau, M. Robert, *ACS Catal.* **2018**, *8*, 3411–3417.
- [36] C. Costentin, S. Drouet, G. Passard, M. Robert, J.-M. Savéant, *J. Am. Chem. Soc.* **2013**, *135*, 9023–9031.

P. Gotico, B. Boitrel, R. Guillot,
M. Sircoglou, A. Quaranta, Z. Halime,*
W. Leibl, A. Aukauloo* — ■■■■-■■■■

Second-Sphere Biomimetic Multipoint
Hydrogen-Bonding Patterns to Boost CO₂
Reduction of Iron Porphyrins



Like CODH: Urea groups at an iron porphyrin catalyst give multipoint hydrogen-bonding stabilization resembling that found in the CO₂ adduct of carbon monoxide dehydrogenase (CODH). The catalyst gave improved CO₂ reduction to CO. Entrapped water molecules within the molecular clefts were found to be the source of protons for the CO₂ reduction.

Accepted manuscript